scientific reports

Check for updates

OPEN

Effect of $C_2H_2F_4/CF_4O$ with low global warming potentials on SiN_x etching as a CHF_3 replacement

Kyung Lim Kim[1,2,9], Jong Woo Hong[3,9], Young Woo Jeon[4], Jun Won Jeong[5], Chan Ho Kim[6], Hyeong Joon Eoh[6], Sung Hyun Kim[3], Jong Soon Park[1,2], Nam Il Cho[1,2], Jung Hun Kwak[7], Yongil Kim[8]✉ & Geun Young Yeom[3,4]✉

As the size of the device continues to decrease due to the increasing demand for faster processing speed and lower power consumption in semiconductor integrated circuit device technology, the double patterning process is widely used. The SiN_x used in this double patterning process requires high etch rate and high etch selectivity over SiO_x, while at the same time achieving an anisotropic etch profile. In the past, gases such as CHF_3/CF_4 were used for SiN_x etching of double patterning. However, the low etch selectivity of these gases and their high global warming potential (GWP) have led to the need for alternative gases. To address this issue, in this study, the effect of alternative gases instead of CHF_3 on SiN_x etching characteristics has been investigated. When $C_2H_2F_4$ was used instead of CHF_3, both etch rate and etch selectivity were improved, but issues such as trenching and increased critical dimension (CD) were observed. When CF_4O was added to $C_2H_2F_4$, both etch rate and etch selectivity were further improved while eliminating trenching issue. The analysis showed that $C_2H_2F_4$ compared to CHF_3 promoted stronger polymer formation, thereby improving mask passivation while trenching defects occurred due to polymer deposition. For the $C_2H_2F_4 + CF_4O$ mixture, increased fluorine dissociation resulted in higher SiN_x etch rates and consequently better etch selectivity, and trenching was eliminated by increasing gas dissociation and decreasing polymer production. Million Metric Tones of Carbon Equivalent (MMTCE) measurements showed that $C_2H_2F_4$ decreased by approximately ~83.9% and $C_2H_2F_4 + CF_4O$ by approximately ~75.2% of greenhouse gas emissions compared to CHF_3. Therefore, the results obtained with alternate gases are next-generation eco-friendly etch processes that can be applied to semiconductor devices such as Fin Field Effect Transistor (FinFET), 3D Not-AND (NAND), and other advanced semiconductor and display manufacturing technologies.

Keywords SiN_x, SiO_x, CF_4O, $C_2H_2F_4$, CHF_3, Global Warming Potential, Dry Etching, Double Patterning

Today, SiN_x and SiO_x offer high performance at low cost with excellent insulating properties and high breakdown strength[1–5]. These advantages have led to their widespread use in applications such as Fin Field-Effect Transistors (FinFETs) and Not-AND (NAND) that require high electrical performances[6–11]. In recent years, the size of devices has been steadily decreasing due to the continuous increase in demand for faster processing speeds and lower power consumption, and, to reduce device sizes below the photolithography wavelength limit, double patterning techniques are widely used[12,13]. The double patterning process requires a highly selective etching process by using an insulated upper hard mask instead of amorphous carbon layer (ACL) or bottom anti-reflective coating (BARC) layer[2,14–17]. This allows for the removal of unnecessary bottom layers through high etch selectivity, reducing process time and double patterning defects, leading to cost savings. In particular,

[1]Department of Semiconductor and Display Engineering, Sungkyunkwan University, Suwon 16419, Republic of Korea. [2]Samsung Institute of Technology, Samsung-Ro 1, Giheung-Gu, Yongin-Si, Gyeonggi-Do 17113, Republic of Korea. [3]School of Advanced Materials Science and Engineering, Sungkyunkwan University (SKKU), Suwon, Gyeonggi-Do 16419, Republic of Korea. [4]Department of Display Engineering, Sungkyunkwan University (SKKU), Suwon, Gyeonggi-Do 16419, Republic of Korea. [5]Department of Semiconductor Convergence Engineering, Sungkyunkwan University (SKKU), Suwon, Gyeonggi-Do 16419, Republic of Korea. [6]SKKU Advanced Institute of Nanotechnology (SAINT), Sungkyunkwan University (SKKU), Suwon, Gyeonggi-Do 16419, Republic of Korea. [7]Research & Development Department Team, SK Specialty, 130, Myeonghaksandan-RoSejong-Si 30068, Yeongdong-Myeon, Republic of Korea. [8]College of Information and Communication Engineering, Sungkyunkwan University (SKKU), Suwon, Gyeonggi-Do 16419, Republic of Korea. [9]These authors contributed equally: Kyung Lim Kim and Jong Woo Hong. ✉email: yikim11@skku.edu; gyyeom@skku.edu

increasingly complex and precise semiconductor etch processes require deeper SiN_x etching than ever before, requiring high etch selectivity between SiN_x and SiO_x[18–25]. This is because employing a highly selective etching process between SiN_x and SiO_x can effectively eliminate the multiple etching steps that are typically required in conventional double patterning techniques. Therefore, the objective of this study is to enhance process efficiency through the implementation of highly selective etching between SiN_x and SiO_x, which removes the necessity for multiple etching sequences commonly employed in traditional double patterning approaches.At present, SiN_x is etched using gases with high global warming potential (GWP) gases such as NF_3/O_2, $CHF_3/O_2/Ar$, $CHF_3/CH_3F/CH_2F_2/Ar$, $N_2/O_2/CF_4$, $SF_6/H_2/He/Ar$ as etchants[16,26–28]. However, CHF_3, CF_4, SF_6, and NF_3have high GWPs. With the development of next-generation etch processes, these high GWP gases must be replaced by lower GWPs[29–32]. To address this issue, a relatively low GWP gas, $C_2H_2F_4$ (HFC-134a), is being considered as a potential alternative to CHF_3. However, it is still high and needs further improvement.In this study, the applicability of $C_2H_2F_4$ to SiN_x etch process as a replacement of CHF_3 using inductively coupled plasma (ICP) during the double patterning process that requires selective etch compared to SiO_x and highly anisotropic etch profiles has been investigated, and, in addition, the effect of CF_4O addition to $C_2H_2F_4$ on the SiN_x etch characteristics has been studied. Because CF_4O helps suppress excessive polymer formation and improve profile control, it was added to $C_2H_2F_4$. Its low GWP, combined with its ability to increase F and O radicals in the plasma, makes it an effective additive for enhancing SiN_x etching performance while reducing environmental impact. First, it was shown that replacing CHF_3 with $C_2H_2F_4$ improves etch selectivity over SiO_x; however, it also resulted in an undesirable increase in critical dimension (CD) and the formation of etch profile defects such as trenching, which are considered negative effects in terms of pattern fidelity and process reliability. However, the addition of CF_4O solved these etch issues, further improving etch rate and selectivity. In addition, Fourier transform infrared spectroscopy (FT-IR) analysis showed that SiN_x etch processes with $C_2H_2F_4$ containing CF_4O improved Million Metric Tons of Carbon Equivalent (MMTCE) values when etching SiN_x of the same thickness compared to conventional CHF_3 processes.

Experimental

The 300 mm inductively coupled plasma (ICP) system used in the study is shown in Fig 1(a). The ICP source consists of an antenna consisting of two copper coils, one inside and one on the outside. A ~35mm thick alumina window was installed above the electrode to pass the electromagnetic field formed from the antenna into the chamber, and in addition to a gas ring located at the top edge of the chamber wall for injecting gas from the side, a gas hole was made in the center of the alumina window for uniform gas distribution in both the center and the edge. The substrate was placed on the powered lower electrode of the ICP system, which was equipped with active cooling using a chiller system. The distance between the substrate surface (placed on the powered lower electrode) and the ICP source region was approximately ~15 cm. The ICP power to the antenna is delivered by a 13.56 MHz radio frequency (RF) generator (Seren-R3001), and the bias power to the substrate is supplied by a 2 MHz RF generator (Seren-R2001). To regulate the process pressure, the chamber is equipped with an automatic process pressure controlling pendulum valve (VAT model PM.7) between the turbopump and the dry pump. At the downstream of the dry pump, an FT-IR (MIDAC, I2000) was installed to measure the recombination gas species. The experiment was performed with a sample of SiN_x (200nm) patterned with SiO_x (110nm) on a silicon wafer. The critical dimension (CD) of the SiO_x hardmask was ~73 nm and the space between patterns was ~71 nm. A SEM cross-sectional image of SiO_x patterned on SiN_x is shown in Fig 1(b). The SiO_x patterned SiN_x etch process was performed under the conditions of an ICP source power of 1500 W with 13.56 MHz RF power, a DC bias of −100 V with the 2 MHz RF power, a process pressure of 4 mTorr, and a substrate temperature of 18 °C. The total gas flow rate was maintained at 340 sccm, consisting of CH_3F (40 sccm), O_2 (90 sccm), and He (100 sccm) supplied in common, together with either CHF_3 (110 sccm), $C_2H_2F_4$ (110 sccm), or a mixture of $C_2H_2F_4$ (80 sccm) + CF_4O (30 sccm) as the main etchant gas. The etch rate and selectivity, and the etch profile of SiO_x patterned SiN_x were examined using the field emission scanning electron microscope (FE-SEM; Hitachi, S-4700), and SEM was also used to measure CD. The plasmas produced by the dissociation of hydrofluorocarbon (HFC) and perfluorocarbon (PFC) gases were observed by optical emission spectroscopy (OES; ANDOR, Technology SR-ASZ-0103). In addition, radicals and cations were measured using quadrupole mass spectrometry (QMS;

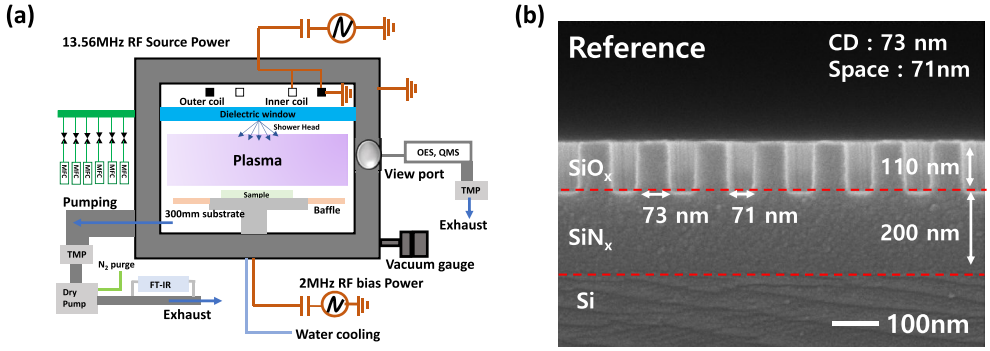

Fig. 1. (**a**) Schematic diagram of the 300 mm ICP system used in the experiment. (**b**) a SEM image of SiO_x masked SiN_x/Si wafer structure used in the experiment.

Hiden Analytical, PSM 500). The surface composition and binding states were measured by X-ray photoelectron spectroscopy (XPS; VG Microtech Inc. ESCA2000). Fourier transform infrared spectroscopy (FT-IR; MIDAC, I2000) was used to measure the molecular species emitted outside of the process chamber and to calculate the total global warming potential of the process gases, Million Metric Tons of Carbon Equivalent (MMTCE) values, used in the experiment.

Results and discussion

SiN_x/SiO_x etching

Fig 2 (a)-(c) show the etch rates and etch selectivity of SiN_x over SiO_x for each etch gas such as (a) 110 sccm CHF_3, (b) 110 sccm $C_2H_2F_4$, and (c) 80 sccm $C_2H_2F_4$+ 30 sccm CF_4O measured as a function of O_2 flow rate. The process conditions were source power 1500 W, DC bias −100 V, process pressure 4 mTorr, and substrate temperature 18° C. CH_3F (40 sccm) and He (100 sccm) were commonly supplied to the chamber. In the case of CHF_3, as shown in Fig 2 (a), etch rates of both SiN_x and SiO_x decreased with increasing O_2 flow rate possibly due to the decreasing etching species in the plasma but the SiN_x etch rate decreased faster possibly due to the oxidation of SiN_x surface, therefore, the etch selectivity of SiN_x over SiO_x decreased with increasing O_2 flow rate and the highest etch selectivity of ~ 3 was observed at 30 sccm O_2 flow rate. In the case of C_2H_2F4, as shown in Fig 2(b), the etch rates of both SiN_x and SiO_x increased with increasing O_2 flow rate. Due to the faster increase of SiO_x etch rate with O_2 flow rate, the etch selectivity of SiN_x over SiO_x was decreased. The further increase of etch rates of SiN_x and SiO_x with increasing O_2 flow rate appears to be related to the removal of a fluorocarbon polymer layer formed by carbon-rich $C_2H_2F_4$ by increased O in the plasma. When 30 sccm CF_4O was mixed with 80 sccm $C_2H_2F_4$ as shown in Fig 2 (c), the etch rates of both SiN_x and SiO_x were higher than 110 sccm $C_2H_2F_4$ at 30 sccm of O_2 possibly due to lower fluorocarbon polymer on the surfaces of materials. And the further increase of O_2 flow rate did not change the SiN_x etch rate significantly while decreasing SiO_x etch rate slightly, therefore, the etch selectivity of SiN_x over SiO_x was slightly increased with increasing O_2 flow rate. (Additional optimization results are presented in the Supplementary Information Figure S1. Although the highest etch rate was observed under one condition, this setting caused reduced SiN_x/SiO_x selectivity and profile degradation. Therefore, the condition that provided a better balance among etch rate, anisotropy, and selectivity was chosen as the optimized condition.) As a result, the SiN_x etch rate and the etch selectivity of SiN_x over SiO_x were the highest as ~ 160 nm/min and ~ 4, respectively, at 30 sccm CF_4O + 80 sccm $C_2H_2F_4$. Therefore, it was found that, for the etching of SiN_x selective to SiO_x, CHF_3-based gas can be replaceable by $C_2H_2F_4$ and, especially, by $C_2H_2F_4$+CF_4O with higher SiN_x etch rate with higher etch selectivity over SiO_x. Also it should be noted that the etch rate and selectivity improvements observed in this study are not solely due to the use of low GWP gases ($C_2H_2F_4$ and CF_4O). The addition of O_2, He, and CH_3F also plays an essential role: O_2 reduces excessive polymer formation, He stabilizes plasma and enhances etch uniformity, and CH_3F contributes to controlled sidewall passivation. These gases, together with the low GWP etchants, collectively determine etch characteristics. To confirm repeatability, the etching experiments were repeated on three separate wafer batches, and the variation in SiN_x/SiO_x etch selectivity was within ±3%, indicating high process reliability.Fig 3 (a)~(c) show SEM cross-sectional images of SiO_x masked SiN_x etch profile after etching ~ 50 nm deep SiN_x, which is generally required for SiN_x etch depth in conventional double patterning process. Etch gases were **(a)** CHF_3 (110 sccm), (b) $C_2H_2F_4$ (110 sccm), and (c) $C_2H_2F_4$(80 sccm)+CF_4O (30 sccm) and the other process conditions were the same as those in Fig 2. As shown in Fig 3(a), for SiN_x etching with CHF_3-based gas, SiO_x mask was consumed the most among three gases in (a)~(c) also, slight SiN_x sidewall etching was observed. When $C_2H_2F_4$ or $C_2H_2F_4$+CF_4O was used instead of CHF_3, as shown in Fig 3(b) and (c), respectively, highly anisotropic SiN_x etch profile with the smaller SiO_x mask etching than CHF_3 in (a) could be observed. However, in general, for the etching of ~50 nm deep SiO_x masked SiN_x etching, three etch gases were applicable for current double patterning process.

Next generation double patterning process requires deeper SiN_x etching, therefore, the etch time was increased to etch ~200 nm thick SiN_x, and the results are shown in Fig 3 (d) CHF_3, (e) $C_2H_2F_4$, and (f) $C_2H_2F_4$+CF_4O[13,16,28,33,34]. For etching with CHF_3-based gas, as shown in Fig 3(d), it was difficult to etch ~ 200 nm deep SiN_x while shrinking CD size significantly and removing SiO_x mask almost completely, due to the

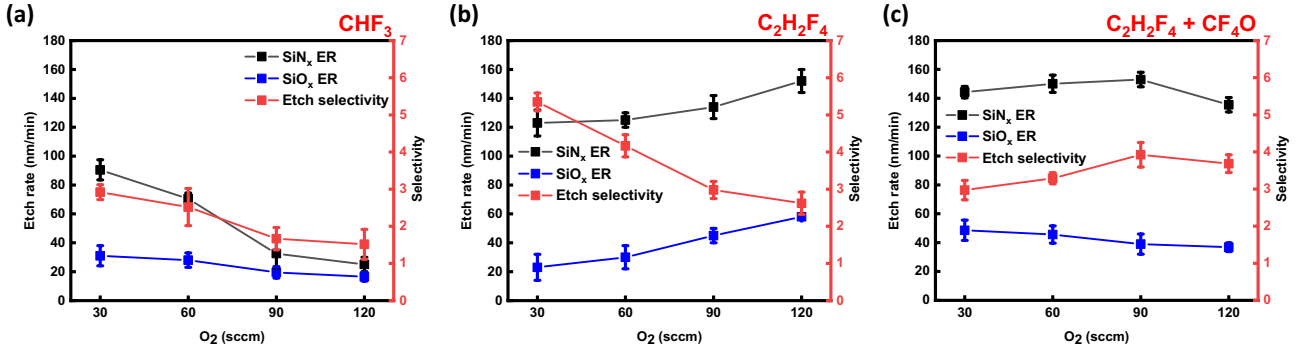

Fig. 2. Etch rate and SiN_x/SiO_x ratio as a function of O_2 flow rate; (**a**) CHF_3 (110 sccm), (**b**) $C_2H_2F_4$ (110 sccm) and (**c**) $C_2H_2F_4$ (80 sccm)+CF_4O (30 sccm). (Additionally, 40 sccm CH_3F and 100 sccm He were added commonly).

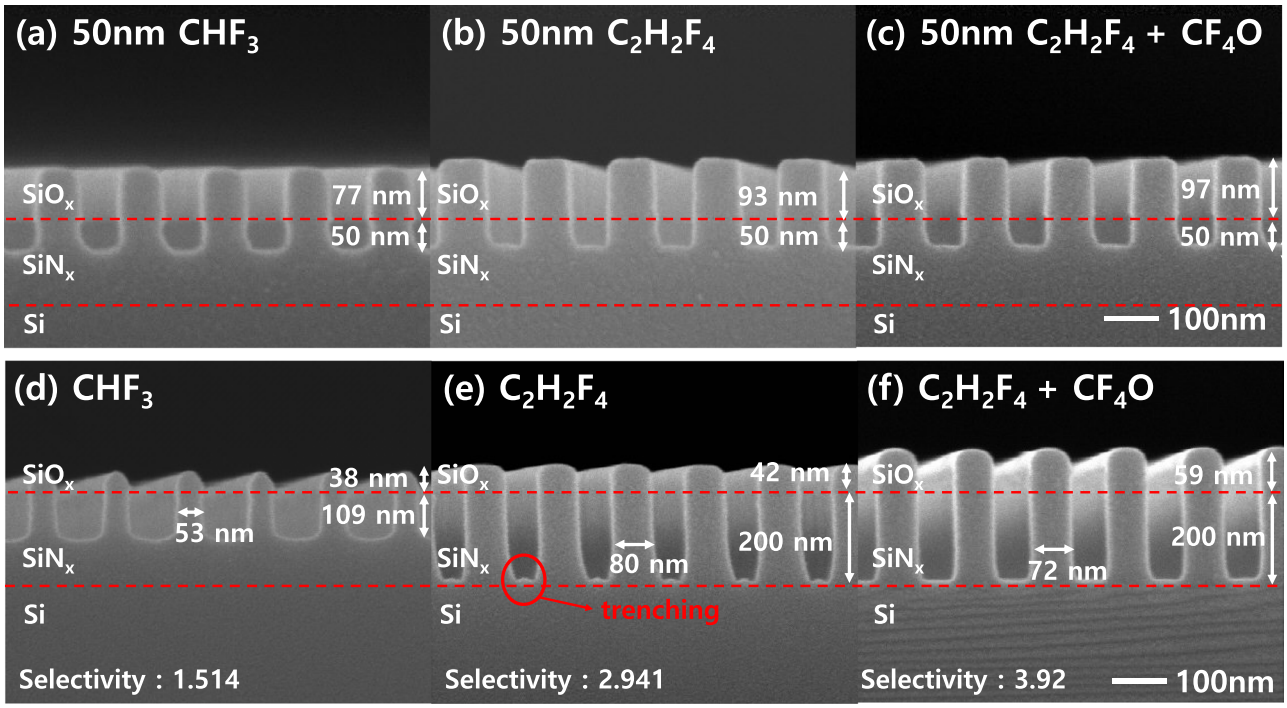

Fig. 3. SEM images of 50nm depth partial SiN_x etch with (**a**) CHF_3 (110 sccm), (**b**) $C_2H_2F_4$ (110 sccm), and (**c**) $C_2H_2F_4$(80 sccm)+CF_4O (30 sccm). SEM images for 200nm depth SiN_x full etching with (**d**) CHF_3, (**e**) $C_2H_2F_4$, and (**f**) $C_2H_2F_4$+CF_4O. The other process conditions are the same as those in Fig 2.

surface oxidation of SiN_x at 90 sccm of O_2 flow rate. (When the O_2 flow rate was decreased to 30 sccm, as shown in Supplementary Information Figure S2, full 200 nm deep SiN_x could be etched with CHF_3-based gas even though the CD size was decreased and SiO_x mask was almost removed similar that at 30 sccm O_2 flow rate.) In the case of $C_2H_2F_4$ and $C_2H_2F_4$+CF_4O, as shown in Fig 3 (e) and (f), respectively, ~ 200 nm deep SiN_x could be fully etched and almost vertical etch profiles were observed. However, in the case of $C_2H_2F_4$-based gas, the CD size was slightly increased and trenching was observed at the etched SiN_xpattern bottom edge possibly due to a polymer layer formed at the pattern bottom. This trenching behavior appears to be in good agreement with previous reports, which suggest that similar profile defects observed in fluorocarbon plasmas may result from localized polymer deposition[17,35]. However, for $C_2H_2F_4$+CF_4O-based gas, vertical SiN_x etch profiles without CD variation and without trenching defects could be observed possibly due to the effective polymer layer removal on the pattern bottom area by addition of CF_4O. As shown in Fig 3 (d-f), replacing CHF_3 with $C_2H_2F_4$ improved the SiN_x/SiO_x selectivity. Moreover, the addition of CF_4O further enhanced the selectivity, which can be attributed to the increased availability of fluorine radicals required for SiN_x etching and the simultaneous suppression of excessive polymer deposition by oxygen radicals. These improvements demonstrate that CF_4O plays a critical role in achieving both anisotropic etching and higher selectivity. Additionally, the sidewall angle could not be measured for the CHF_3-based process due to the incomplete etching of the SiN_x layer. For the $C_2H_2F_4$-based process, the measured sidewall angle was approximately ~84°, while for the $C_2H_2F_4$+CF_4O-based process, it was around ~88°, confirming highly anisotropic and vertical etch profiles. The etch uniformity across the wafer was maintained within ±5%.

Plasma analysis

Using the process conditions in Fig 3, the dissociated species in the plasma were observed using QMS and OES. Fig 4 (a) and (b) show positive ion species in the plasma and their relative intensities, respectively, measured by QMS. (Total measured ion intensities were measured and the results are shown in Supplementary Information Figure S3 and the total ion intensities were the highest for CHF_3-based gas and the lowest for $C_2H_2F_4$-based gas possibly indicating the lowest plasma density for the $C_2H_2F_4$-based gas.) Fig 4 **(a)** shows an overview of the positive ion species detected in the plasma for each gas chemistry, as measured by QMS. As shown in Fig 4 (b), polymerizing ion species such as CH_2F^+, CHF_2^+, and $C_2H_2F_3^+$ were slightly more abundant in the CHF_3-based plasma compared to $C_2H_2F_4$ and $C_2H_2F_4$+CF_4O plasmas, which showed similar levels. In addition, the CHF_3 plasma exhibited the highest O_2^+ ion intensity, whereas the lowest O_2^+ intensity was observed with the $C_2H_2F_4$-based plasma, indicating a stronger oxidation potential in the CHF_3 condition. The largest amount of O_2^+ in the plasma for CHF_3-based gas is believed to be related to the oxidation of SiN_x while the lowest O_2^+ amount in the plasma for $C_2H_2F_4$-based gas is related to the trenching of the patterned SiN_x edge due to the polymer formed on the pattern surface. Etch species such as HF^+ and CF_3^+ were the highest for $C_2H_2F_4$+CF_4O and the lowest for CHF_3^+, and which is believed to be partially related to the highest SiN_x etch rate for $C_2H_2F_4$+CF_4O and the lowest for the CHF_3.Fig 4 (c) shows the OES wide scan data for CHF_3, $C_2H_2F_4$, and $C_2H_2F_4$+CF_4O-

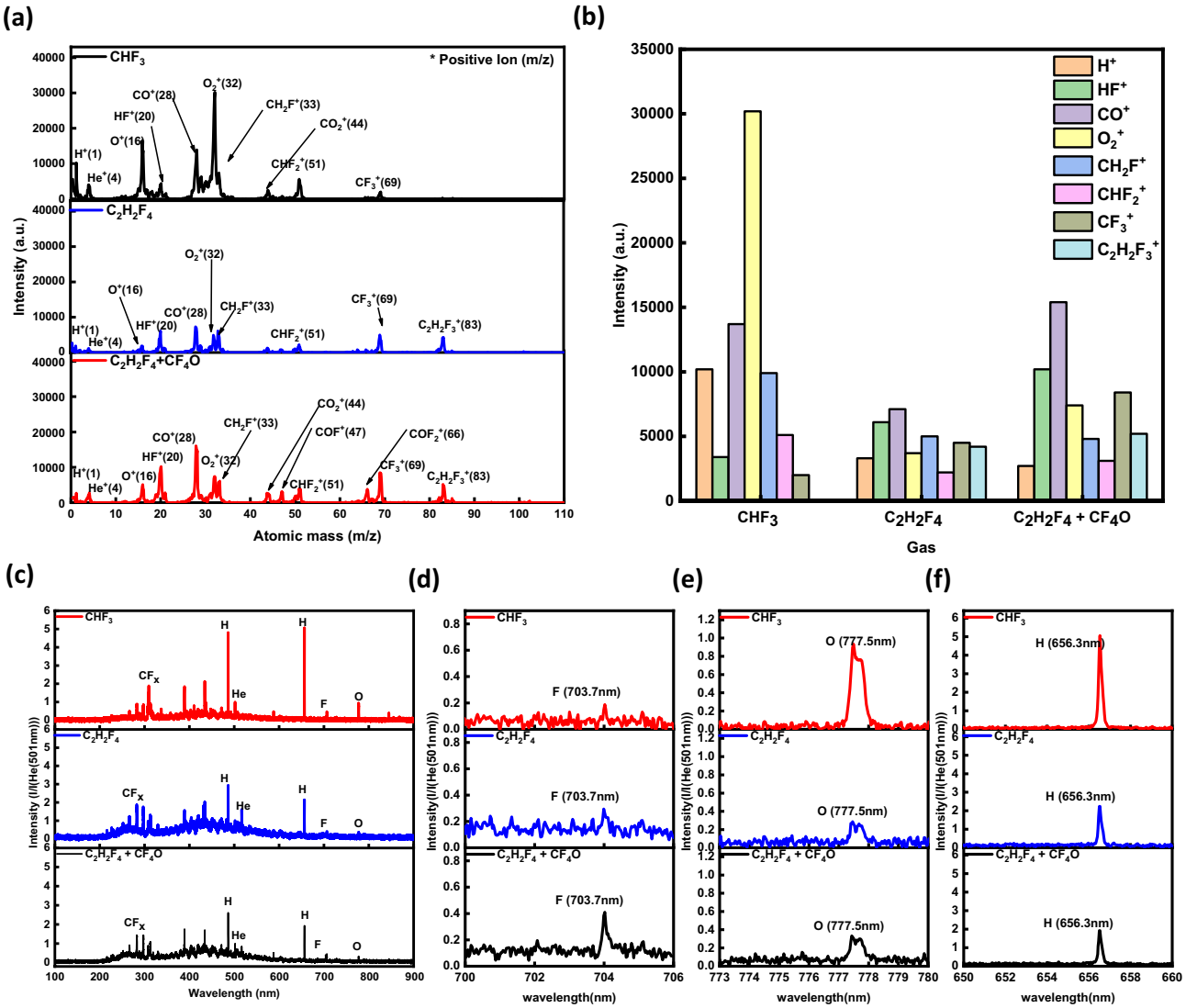

Fig. 4. (**a**) Positive ions in the plasmas by QMS formed using CHF_3, $C_2H_2F_4$, and $C_2H_2F_4$+CF_4O-based gas in Fig 3. (**b**) Intensities of each positive ion. (**c**) OES wide scan data for CHF_3, $C_2H_2F_4$, and $C_2H_2F_4$+CF_4O-based gas in Fig 3. OES narrow scan data related to (**d**) F, (**e**) O, and (**f**) H normalized by He.

based gas in Fig 3 and (d)~(f) show OES narrow scan data related to (d) F (703.7 nm), (e) O (777.4 nm), and (f) H (656.5 nm)[30,31,36–38]. The peak intensities were normalized by He (501.6 nm) peak intensity. The intensity variation of O and H observed by OES were similar to the variation of those positive ion mass intensities (for O, CHF_3>>$C_2H_2F_4$+CF_4O>$C_2H_2F_4$ and for H, CHF_3>$C_2H_2F_4$>$C_2H_2F_4$+CF_4O) The highest O_2^+ ion intensity was observed in the CHF_3-based plasma, which is associated with enhanced oxidation and suppression of polymer accumulation. In contrast, the lowest O_2^+ level in $C_2H_2F_4$-based plasma results in reduced oxidation, promoting polymer formation and the occurrence of trenching. In addition, using OES, the variation of F peak intensity in the sequence of $C_2H_2F_4$+CF_4O>$C_2H_2F_4$>CHF_3 could be observed, and which is believed to be related to the SiN_x etch rate together with variation of CF_3^+ and HF^+ observed by QMS.

Surface analysis & etch mechanism

The atomic composition of the etched SiN_x and SiO_x surfaces and the binding states of Si under the process conditions in Fig 3 were measured by XPS, which are shown in Fig 5. All plasma and surface characterizations in this study were conducted on blanket wafers. As such, sidewall-specific effects in patterned features are not directly assessed. To minimize surface contamination, the etched samples were vacuum-packed to reduce exposure to air and then transferred to the XPS chamber. The measurements were carried out under high vacuum conditions (~10^{-9}Torr). For the XPS analysis, the SiN_x and SiO_x were etched for 2 min. Fig 5 (a) and (b) show the atomic composition of the etched SiN_x and SiO_x surfaces, respectively. As shown in Fig 5(a), the SiN_x surface has the most C percentage for $C_2H_2F_4$-based gas, followed by $C_2H_2F_4$+CF_4O, and then CHF_3, while O percentage has the most for CHF_3, followed by $C_2H_2F_4$+CF_4O, and $C_2H_2F_4$. Therefore, it is believed that the SiN_x surface etched by CHF_3-based gas was oxidized due to the highest O percentage while the SiN_x surface etched

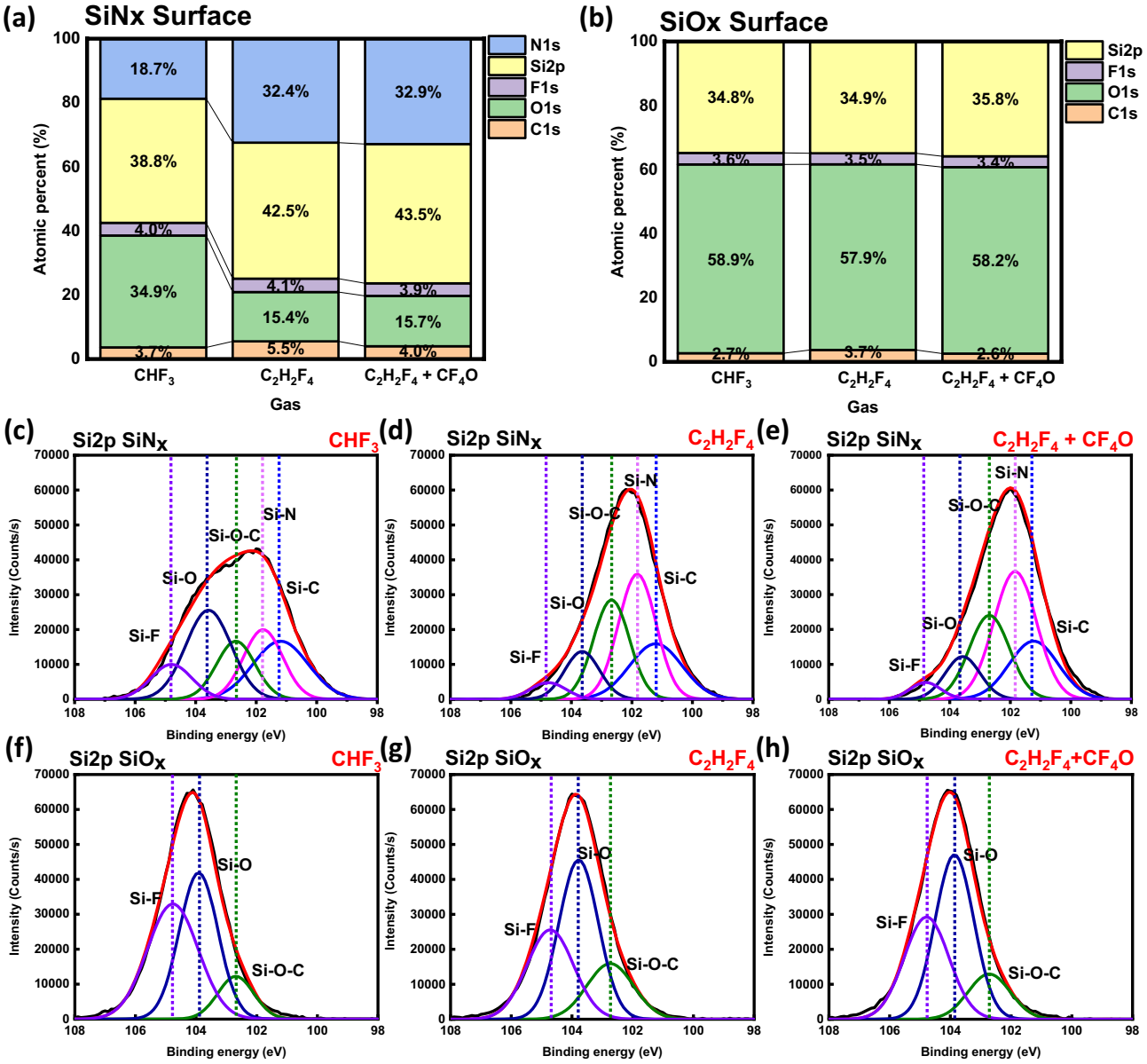

Fig. 5. Atomic percentages of (**a**) SiN_x and (**b**) SiO_x surfaces measured by XPS after etching using the process conditions in Fig 3. XPS Si 2p narrow scan data on etched SiN_x for (**c**) CHF_3, (**d**) $C_2H_2F_4$, and (**e**) $C_2H_2F_4$+CF_4O and XPS Si 2p narrow scan data on etched SiO_x for (**f**) CHF_3, (**g**) $C_2H_2F_4$, and (**h**) $C_2H_2F_4$+CF_4O.

by $C_2H_2F_4$ was polymerized due to the highest C percentage. In addition, the higher percentages of Si and N in the order of CHF_3, $C_2H_2F_4$, and $C_2H_2F_4$+CF_4O appear to be related to the etch rate of SiN_x. In contrast, the etched SiO_x surfaces, as shown in Fig 2(a)–(c), exhibit similar etch rates regardless of gas chemistry, suggesting that the underlying etching mechanism remains consistent across the different plasma conditions. The surface characteristics were further investigated by observing XPS narrow scan data of Si 2p for the SiN_x and SiO_x etched with CHF_3, $C_2H_2F_4$, and $C_2H_2F_4$+CF_4O. The results are shown in Fig 5(c) CHF_3, (d)$C_2H_2F_4$, and (e) $C_2H_2F_4$+CF_4O for etched SiN_x surface and (f) CHF_3, (g)$C_2H_2F_4$, and (h)$C_2H_2F_4$+CF_4O for etched SiO_x surface. As shown in Fig 5 (c~e), the SiN_x etched with CHF_3 showed the highest Si-O bonding (~103.6 eV)[39] while the SiN_x etched with $C_2H_2F_4$ and $C_2H_2F_4$+CF_4O showed the highest Si-N bonding (~101.8 eV)[40] indicating the oxidation of SiN_x surface by CHF_3, which results in low SiN_x etch rate. (Supplementary Information Figure S4 shows XPS C1s narrow scan data for SiN_x and SiO_x etched with CHF_3, $C_2H_2F_4$, and $C_2H_2F_4$+CF_4O. Both SiN_x and SiO_x surfaces etched with $C_2H_2F_4$ showed the highest C–F (~289.5 eV), C–CF (~287.5 eV), and C–CF_2 (~291.8 eV) bondings related to a fluorocarbon polymer layer, and $C_2H_2F_4$+CF_4O exhibited slightly lower intensities, while CHF_3 showed the lowest among the three gases. Therefore, SiN_x etched with $C_2H_2F_4$ exhibited the thickest polymer layer on the etched SiN_x surface, and which might be related to the trenching of etched SiN_x pattern edge.) In the case of SiO_x surfaces, as shown Fig 5 (f~h), Si-O bonding (~103.6 eV) was the highest binding peaks

for all the three gases, therefore, no significant differences in SiO_x etch rate could be observed. (Supplementary Information Figure S5 shows the atomic percentages of SiN_x and SiO_x surfaces measured by XPS after etching using CHF_3 with 30 sccm of O_2 flow rate, and XPS Si 2p and C1s narrow scan data on SiN_x and SiO_x surfaces etched using CHF_3 with 30 sccm of O_2 flow rate. The use of 30 sccm O_2 flow rate for the etching of SiN_x and SiO_x with CHF_3 decreased the O percentage and Si-O bonding peak on the etched SiN_x surface similar to those for the SiN_x etched using $C_2H_2F_4$ and $C_2H_2F_4$+CF_4O with 90 sccm O_2 flow rate while no significant change was observed for the etched SiO_x surface similar to the surface etched with 90 sccm O_2 flow rate.)Fig 6(a)~**(c)** shows the potential etch mechanism of SiO_x masked SiN_x pattern etching under the process conditions in Fig 3. Fig 6(a) shows the etch behavior of SiN_x when using CHF_3 gas. During the etching process with CHF_3, surface oxidation occurs on SiN_x surface, resulting in significant decrease of SiN_x etching. Fig 6(b) shows the SiN_x etching process using $C_2H_2F_4$ gas. The low surface oxidation of SiN_x maintains etching, enabling full etching with a thickness of ~ 200 nm. However, the formation of a polymer layer in the SiN_x pattern due to $C_2H_2F_4$ leads to problems such as tapered profile and trenching. Fig 6(c) shows the etching mechanism under the $C_2H_2F_4$+CF_4O. The addition of CF_4O reduced polymer formation, resulting in higher etching rates and better selection ratios compared to $C_2H_2F_4$ alone, eliminating trenching within the SiN_x pattern. Consequently, the trenching and tapered profiles observed under $C_2H_2F_4$-based plasma are primarily caused by excessive fluorocarbon polymer deposition, which disrupts uniform ion flux toward the pattern bottom. The incorporation of CF_4O promotes the oxidation of carbon-based species, thereby reducing polymer thickness and improving etch anisotropy.

Measurement of million metric tons of carbon equivalents

Table 1 provides detailed information including the names of the gases used in the experiment, their molecular weights, GWP values and the Chemical Abstracts Service (CAS) values. CHF_3 exhibits a high global warming potential ($GWP100_{yr}$) value of 14,600, $C_2H_2F_4$ shows a $GWP100_{yr}$ value of 1,430, and CF_4O represents a very low $GWP100_{yr}$ value close to ~1[41]. However, since the gases used in etching have the potential to recombine and form by-products after decomposition during plasma discharge, it is essential to analyze the gas concentration in the exhaust line and calculate the Million Metric Tons of Carbon Equivalent (MMTCE), which corresponds to the total global warming index. Below is the equation for the MMTCE. The MMTCE was calculated using $GWP100_{yr}$, which refers to the integrated global warming potential over a 100-year time horizon, while *Mi* represents the total mass emission of HFCs and PFCs measured by FT-IR during the process[42]

$$\mathrm{MMTCE} = \sum_i \frac{12}{44} \times \frac{\boldsymbol{M_i} \times \boldsymbol{GWP}_{100\boldsymbol{yr}}}{10^9}$$

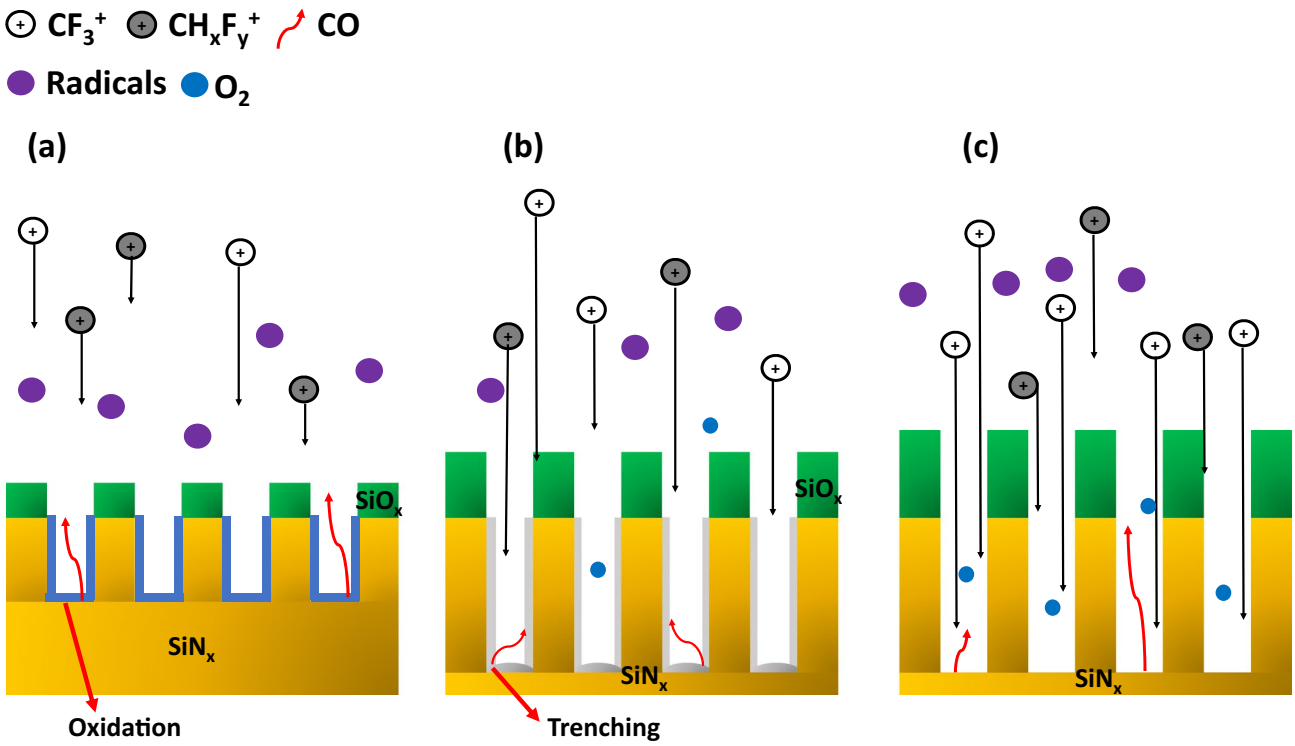

Fig. 6. Schematic drawings of etch mechanism for SiO_x masked SiN_x etching with CHF_3, $C_2H_2F_4$, $C_2H_2F_4$+CF_4O-based gases. (**a**) for CHF_3-based gas, due to the SiN_x oxidation, the etching of SiN_x is very slow. (**b**) for $C_2H_2F_4$-based gas, due to the polymer formation, trenching is formed at the SiN_x pattern bottom edge. (**c**) for $C_2H_2F_4$+CF_4O, the polymer layer in the pattern is effectively removed and highly anisotropic SiN_x etching is obtained.

Gas name	Molecular formula	Molecular weight (g/mol)	GWP 100$_{yr}$	CAS number
Trifluoromethane (HFC-23)	CHF_3	70.03	14,600	75-46-7
1,1,2,2-Tetrafluoroethane (HFC-134)	$C_2H_2F_4$ (CHF_2CHF_2)	102.03	1,430	359-35-3
Trifluoromethyl hypo fluorite	CF_4O (CF_3OF)	104.004	~ 1	373-91-1

Table 1. Information on CHF_3, $C_2H_2F_4$, and CF_4O used in the experiment (e.g., gas name, molecular weight, GWP 100 years, and CAS number).

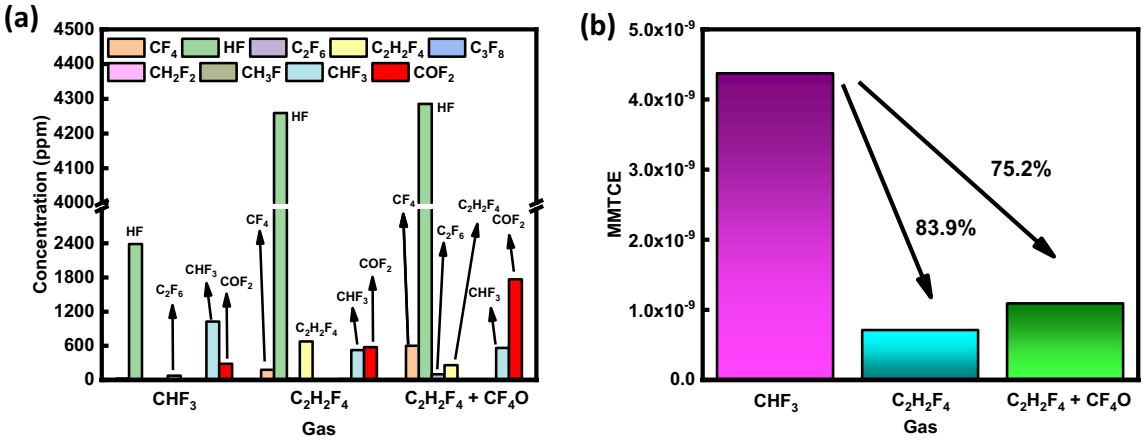

Fig. 7. (**a**) Concentration of exhaust gases (ppm) measured using FT-IR in the exhaust line during plasma generation using CHF_3, $C_2H_2F_4$, $C_2H_2F_4$+CF_4O-based in Fig 3. (**b**) MMTCE values calculated for the gases used to etch the same SiN_x thickness.

Fig 7(a) shows the concentration (in ppm) of exhaust gases measured in the exhaust line using FT-IR during plasma generation using CHF_3, $C_2H_2F_4$, and $C_2H_2F_4$+CF_4O-based gas under the process conditions in Fig 3, and which shows the various recombinants of decomposed etched gases. In the case of CHF_3, recombinants such as HF (GWP = 0), COF_2 (GWP = ~1), and CHF_3 itself were detected along with the formation of C_2F_6(GWP = 12,400), a high GWP gas[41,43]. In the case of $C_2H_2F_4$, more HF and COF_2 with low GWP values were formed compared to CHF_3, while the formation of CHF_3 having a high GWP decreased. Although CF_4(GWP = 7,380) was produced, it was found to be relatively small[44,45]. For $C_2H_2F_4$+CF_4O, the formation of C_2F_6 was also observed compared to $C_2H_2F_4$, and the amount of COF_2 increased. The concentrations of HF and CHF_3 remained similar. However, the addition of CF_4O led to an increase in CF_4 formation during its dissociation and recombination. Fig 7(b) shows the MMTCE graph calculated when etching a ~50 nm high SiN_x target. When $C_2H_2F_4$-based gas was used instead of the conventional CHF_3-based gas, ~83.9% reduction of MMTCE was observed. In the case of using $C_2H_2F_4$+CF_4O-based gas, CF_4 was produced due to CF_4O, resulting in a ~75.2% reduction compared to the conventional CHF_3-based gas. However, the $C_2H_2F_4$+CF_4O -based etch process not only showed higher SiN_x etch rates and etch selectivity of SiN_x over SiO_x but also emitted much lower greenhouse emissions compared to the conventional CHF_3 process, confirming that it is an etching process that can replace the etching process using CHF_3, which is suitable for next-generation applications and is environmentally friendly.

Conclusions

This study investigated etch properties using low global warming potential (GWP) gases as an alternative to CHF_3, which has traditionally been used in SiN_x etch processes selective to SiO_x such as double patterning processes for FinFET, 3D NAND fabrication, etc. Such processes are directly relevant to advanced memory fabrication, where SiN_x is commonly used as a spacer or dielectric layer. These structures require precise profile control, minimization of polymer-induced defects, and compatibility with high-aspect-ratio integration. Replacing CHF_3 with $C_2H_2F_4$ resulted in higher SiN_x etch rates and higher etch selectivity over SiO_x, but trenching phenomena were observed in the etched pattern edge. By replacing it with $C_2H_2F_4$+CF_4O, not only higher SiN_x etch rate but also trenching could be eliminated.Plasma and surface analysis showed that, in the case of etch processing using CHF_3, the SiN_x etch rate was slow due to oxidation of the SiN_x surface due to the large amount of oxygen in the plasma, while in the case of $C_2H_2F_4$, the trenching phenomenon was observed by forming a polymer on the pattern surface. By adding CF_4O to the $C_2H_2F_4$, the polymer formed on the pattern surface could be successfully removed, and not only the SiN_x etch rate was increased, but also the trenching phenomenon was eliminated. In addition, the calculation of MMTCE showed that, when $C_2H_2F_4$ and $C_2H_2F_4$+CF_4O were used instead of conventional CHF_3, the MMTCEs were significantly reduced by ~83.9% and ~75.2%, respectively. These improvements, combined with significantly reduced MMTCE values, suggest that $C_2H_2F_4$+CF_4O is a

promising candidate for eco-friendly and high-precision SiN_x etch processes applicable to advanced FinFET and 3D NAND device fabrication.

Data availability

Data will be made available on request to Yongil Kim (yikim11@skku.edu) and Geun Young Yeom. (gyyeom@skku.edu).

Received: 25 July 2025; Accepted: 13 October 2025
Published online: 18 November 2025

References

1. Sun, Y. *Destruction of Fluorinated Greenhouse Gases by Using Nonthermal Plasma Process*, In: *Planet Earth 2011 - Global Warming Challenges and Opportunities for Policy and Practice, InTech*. https://doi.org/10.5772/23405.
2. Ye, J. H. & Zhou, M.S. *Carbon Rich Plasma-Induced Damage in Silicon Nitride Etch*, 2000.
3. Rentsch, J. et al. *Preu, Plasma Cluster Processing for Advanced Solar Cell Manufacturing*, n.d.
4. Lugani, G. S. et al. Direct Emissions Reduction in Plasma Dry Etching Using Alternate Chemistries: Opportunities, Challenges and Need for Collaboration. *IEEE Trans. Semicond. Manuf.* https://doi.org/10.1109/TSM.2024.3444465 (2024).
5. Kim, T., Shin, D., Park, J., Pham, D. P. & Yi, J. Mobility improvement of LTPS thin film transistor using stacked capping layer. *Microelectron Eng* https://doi.org/10.1016/j.mee.2021.111591 (2021).
6. Guertin, J. P. & Onvszchuk, M. Coordination of silicon tetraBuoside with pyridisae and other nitrogen electron-pair donor molecnPesl. *Can. J. Chem.* **47**(8), 1275–1279 (1969).
7. Mccurdy, B. J. *Matrix Reactions of Silicon Difluoride as Studied by Infrared Spectroscopy*, 1966.
8. Zhou, H., Song, Y., Xu, Q., Li, Y. & Yin, H. Fabrication of Bulk-Si FinFET using CMOS compatible process. *Microelectron Eng* **94**, 26–28. https://doi.org/10.1016/j.mee.2012.01.004 (2012).
9. Chatterjee, S. & Kim, H. Material engineering to enhance reliability in 3D NAND flash memory. *Mater. Today Phys.* **40**, 100928. https://doi.org/10.1016/j.mtphys.2024.100928 (2024).
10. Sevilla, G. A. T. et al. Flexible and transparent silicon-on-polymer based sub-20 nm non-planar 3D FinFET for brain-architecture inspired computation. *Adv. Mater.* **26**, 2794–2799. https://doi.org/10.1002/adma.201305309 (2014).
11. IEEE Staff, *IEEE/SEMI Advanced Semiconductor Manufacturing Conference*, *IEEE*, 2009.
12. Barnola, S. et al. *Integration of dry etching steps for double patterning and spacer patterning processes*, In: *Optical Microlithography XXII, SPIE,*: 72741X. https://doi.org/10.1117/12.814856. (2009).
13. 2018 IEEE International Interconnect Technology Conference (IITC) : 4-7 June 2018, [IEEE], 2018.
14. Hyun, K. D. *Thesis for the Degree of Doctor of Philosophy Low-temperature atomic layer deposition of high-quality SiO2 and Si3N4 thin films*, 2019.
15. Chang, B. Integrated in situ self-aligned double patterning process with fluorocarbon as spacer layer. *J. Vac. Sci. Technol., B: Nanotechnol. Microelectron.: Mater., Process., Meas., Phenom.* https://doi.org/10.1116/6.0000089 (2020).
16. Reyes-Betanzo, C., Moshkalyov, S. A., Swart, J. W. & Ramos, A. C. S. Silicon nitride etching in high- and low-density plasmas using $SF_6/O_2/N_2$ mixtures. *J. Vac. Sci. Technol., A: Vac., Surf. Films* **21**, 461–469. https://doi.org/10.1116/1.1547703 (2003).
17. Kuo, W. C. & Liu, C. M. A plasma processing combined with trench isolation technology for large opening of parylene based high-aspect-ratio microstructures. *Microelectron Eng* **133**, 51–58. https://doi.org/10.1016/j.mee.2014.11.012 (2015).
18. Lill, T. et al. Low-temperature etching of silicon oxide and silicon nitride with hydrogen fluoride. *J. Vac. Sci. Technol., A* https://doi.org/10.1116/6.0004019 (2024).
19. Hsiao, S. N., Britun, N., Nguyen, T. T. N., Sekine, M. & Hori, M. Etching Mechanism Based on Hydrogen Fluoride Interactions with Hydrogenated SiN Films Using HF/H_2 and CF_4/H_2 Plasmas. *ACS Appl Electron Mater* **5**, 6797–6804. https://doi.org/10.1021/acsaelm.3c01258 (2023).
20. Hsieh, S. I. et al. Reliability and memory characteristics of sequential laterally solidified low temperature polycrystalline silicon thin film transistors with an oxide-nitride-oxide stack gate dielectric, *Japanese J. Applied Phys*. Part 1: Regular Papers and Short Notes and Review Papers **45** 3154–3158. https://doi.org/10.1143/JJAP.45.3154. (2006).
21. Huzaibi, H. U. et al. Charge transport mechanism in low temperature polycrystalline silicon (LTPS) thin-film transistors. *AIP Adv* https://doi.org/10.1063/1.5082994 (2019).
22. Kim, J., Kang, H., Kim, Y., Jeon, M. & Chae, H. Low global warming $C_5F_{10}O$ isomers for plasma atomic layer etching and reactive ion etching of SiO_2 and Si_3N_4. *Plasma Processes Polym.* https://doi.org/10.1002/ppap.202300216 (2024).
23. Chen, B. W. et al. Systematic Analysis of High-Current Effects in Flexible Polycrystalline-Silicon Transistors Fabricated on Polyimide. *IEEE Trans Electron Devices* **64**, 3167–3173. https://doi.org/10.1109/TED.2017.2715500 (2017).
24. Gong, L. et al. Investigation of the etching mechanism of silicon nitride by $CF_4/O_2/Ar$ gas mixture plasma in ICP. *Vacuum* **233**, 114000. https://doi.org/10.1016/j.vacuum.2024.114000 (2025).
25. Gil, H. S. et al. Selective isotropic etching of SiO_2 over Si3N4 using NF_3/H_2 remote plasma and methanol vapor. *Sci Rep* https://doi.org/10.1038/s41598-023-38359-4 (2023).
26. Pankratiev, P. et al. Selective SiN/SiO_2 etching by $SF_6/H_2/Ar/He$ plasma, In: *AIP Conf Proc, American Institute of Physics Inc.*, https://doi.org/10.1063/1.5135490. (2019).
27. Ohtake, H., Wanifuchi, T. & Sasaki, M. SiN etching characteristics of $Ar/CH_3F/O_2$ plasma and dependence on SiN film density. *Jpn J Appl Phys* https://doi.org/10.7567/JJAP.55.086502 (2016).
28. Gatzert, C., Blakers, A. W., Deenapanray, P. N. K., Macdonald, D. & Auret, F. D. Investigation of reactive ion etching of dielectrics and Si in CHF_3/O_2 or CHF_3/Ar for photovoltaic applications. *J. Vac. Sci. Technol., A: Vac., Surf. Films* **24**, 1857–1865. https://doi.org/10.1116/1.2333571 (2006).
29. Fracassi, R. F. *D'agostino, Contribution to Global Warming of Plasma Polymerization and Treatment Processes Fed with Fluorinated Compounds**, (1999).
30. Woo Hong, J. et al. Reactive ion etching of indium gallium zinc oxide (IGZO) and chamber cleaning using low global warming potential gas. *Appl Surf Sci* https://doi.org/10.1016/j.apsusc.2024.160692 (2024).
31. Hong, J. W. et al. Indium tin oxide etch characteristics using C_xH_{2x+2}(x=1,2,3)/Ar. *Mater Sci Semicond Process* https://doi.org/10.1016/j.mssp.2023.107395 (2023).
32. Kim, Y. et al. Low Global Warming $C_4H_3F_7O$ Isomers for Plasma Etching of SiO_2 and Si_3N_4Films. *ACS Sustain Chem Eng* **10**, 10537–10546. https://doi.org/10.1021/acssuschemeng.2c01705 (2022).
33. Kwan Lee, H. Soo Chung, H. & Su Yu, J. *Selective Etching of Thick Si3N4 , SiO2 and Si by Using CF4/O2 and C2F6> Gases with or without O2 or Ar Addition*, (2009).
34. Loong, S. Y. et al. *Characterization of polymer formation during Si02 etching with different fluorocarbon gases (CHF3, CF4, C4F8)*, n.d. http://spiedl.org/terms.

35. Kim, S.-W. et al. Analytical study of polymer deposition distribution for two-dimensional trench sidewall in low-k fluorocarbon plasma etching process. *J. Vac. Sci. Technol., B: Nanotechnol. Microelectron.: Mater., Process., Meas., Phenom.* https://doi.org/10.1116/1.4996641 (2018).
36. Hong, J. W. et al. Effect of various pulse plasma techniques on TiO_2 etching for metalens formation. *Vacuum* https://doi.org/10.1016/j.vacuum.2023.111978 (2023).
37. Hong, J. W. et al. Etched characteristics of nanoscale TiO_2 using C_4F_8-based and BCl_3-based gases. *Mater Sci Semicond Process* https://doi.org/10.1016/j.mssp.2023.107617 (2023).
38. Il Cho, N. et al. Etch characteristics of maskless oxide/nitride/oxide/nitride (ONON) stacked structure using $C_4H_2F_6$-based gas. *Sci Rep* https://doi.org/10.1038/s41598-024-74107-y (2024).
39. De Santis, P. Palleschi, A. Savino, M. Scipioni, A. & Moro, C. P. A. *Per lo Studio degli, Poly(DL-prollne), a Synthetic Polypeptide Behaving as an Ion Channel across Membranes:* In *Conformational Studies on Ion Complexes of the Tetramer Boc(D-Pro-L-Pro)2OCH*$_3$. https://pubs.acs.org/sharingguidelines. (1988).
40. Lee, W.-J. Lee, J.-H. Park, C.O. Lee, Y.-S. & Shin, S.-J. *A Comparative Study on the Si Precursors for the Atomic Layer Deposition of Silicon Nitride Thin Films,* 2004.
41. AR6 WGI Report-List of corrigenda to be implemented, n.d. https://github.com/IPCC-WG1/Chapter-7.
42. Lee, H. S. et al. SiO_2 etch characteristics and environmental impact of Ar/C_3F_6O chemistry. *J. Vac. Sci. Technol., A: Vac., Surf. Films* https://doi.org/10.1116/1.5027446 (2018).
43. Victor, D. G. & Macdonald, G. J. *A Model For Estimating Future Emissions of Sulfur Hexafluoride and Perfluorocarbons.* (1999).
44. Rabie, M. & Franck, C. Computational screening of new high voltage insulation gases with low global warming potential. *IEEE Trans. Dielectr. Electr. Insul.* **22**, 296–302. https://doi.org/10.1109/TDEI.2014.004474 (2015).
45. Harvey, R. *Estimates of U.S. Emissions of High-Global Warming Potential Gases and the Costs of Reductions.* http://www.epa.gov/ghginfo. (2000).

Acknowledgements

This work was supported by the Technology Innovation Program Development Program-Development of core technology in Carbon Neutrality (RS-2023-00265858, Development of alternative PFC gas with low GWP value under 150 for OLED display oxide TFT insulator patterning) funded By the Ministry of Trade, Industry & Energy(MOTIE, Korea).

Author contributions

K.L.K and J.W.H contributed to the experimental design. Y.W.J contributed to the experimental setup. J.W.J, C.H.K, H.J.E and S.H.K contributed to the data analysis. J.S.P and N.I.C, J.H.K initiated the project. G.Y.Y and Y.G.K participated in writing the manuscript.

Declarations

Competing interests

The authors declare no competing interests.

Additional information

Correspondence and requests for materials should be addressed to Y.K. or G.Y.Y.